

# RECURSIVE ELIMINATION OF TEMPORAL CONTRASTS BETWEEN TIME-LAPSE ACOUSTIC WAVE FIELDS

M.W.P. DILLEN, J.T. FOKKEMA and C.P.A. WAPENAAR  
Delft University of Technology, Department of Applied Earth Sciences, Delft, the Netherlands

## Abstract

A boundary integral representation of the difference of time-lapse acoustic wave fields is investigated. Recursive computation of the boundary integral eliminates the action of temporal contrast sources above the boundary at which the integral is evaluated. This method is a basis for prestack temporal contrast imaging and inversion schemes, analogous to implementations of the Kirchhoff integral in inverse scattering theory.

## Boundary integral

We consider two sets of time-lapse acoustic wave fields, denoted by *reference* wave fields and *monitor* wave fields, associated with seismic experiments. We assume that the duration of the reference and monitor seismic experiments is much smaller than the time-lapse interval between the two experiments, such that during either seismic experiment the medium parameters, may be approximated by constant functions of time. Reference and monitor wave field quantities, pressure  $p$  and particle velocity  $v_k$ , density  $\rho$  and compressibility  $\kappa$ , and sources  $q$  and  $f_k$ , are denoted by the superscripts  $\cdot^{(1)}$  and  $\cdot^{(2)}$ , respectively. Consider the Fourier domain (signified by  $\hat{\cdot}$ ) acoustic reference and monitor wave field equations,

$$\partial_k \hat{p}^{(1),(2)}(\mathbf{x}, \omega) + j\omega \rho^{(1),(2)}(\mathbf{x}) \hat{v}_k^{(1),(2)}(\mathbf{x}, \omega) = \hat{f}_k^{(1),(2)}(\omega) \delta(\mathbf{x} - \mathbf{x}'), \quad (1)$$

$$\partial_k \hat{v}_k^{(1),(2)}(\mathbf{x}, s) + j\omega \kappa^{(1),(2)}(\mathbf{x}) \hat{p}^{(1),(2)}(\mathbf{x}, \omega) = \hat{q}^{(1),(2)}(\omega) \delta(\mathbf{x} - \mathbf{x}'), \quad (2)$$

with  $\mathbf{x} = (\mathbf{x}_T, x_3) \in \mathbb{R}^3$ , in which  $\mathbf{x}_T = (x_1, x_2)$  denotes the transverse coordinate, and  $x_3$  denotes the longitudinal coordinate, oriented in the main wave field direction. The Fourier transform parameter  $\omega$  is the radial frequency. The space  $\mathbb{R}^3$  is divided by the planar surface,

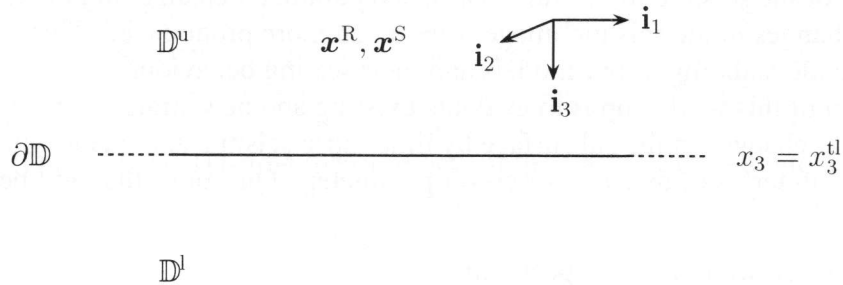


Figure 1: Time-lapse configuration with source positions in upper half-space  $\mathbb{D}^u$ .

$\partial\mathbb{D} = \{(\mathbf{x}_T, x_3) \mid \mathbf{x}_T \in \mathbb{R}^2, x_3 = x_3^{tl}\}$ , into an upper half-space  $\mathbb{D}^u$  and a lower half-space  $\mathbb{D}^l$  (Fig. 1). We consider inside  $\mathbb{D}^u$  the reference and monitor source distributions at  $\mathbf{x}' = \mathbf{x}^R$  and  $\mathbf{x}' = \mathbf{x}^S$ , respectively. We define, omitting the  $\omega$ -dependency, the following interaction integral,

$$\hat{I}^{\text{conv}}(x_3^{tl}; \mathbf{x}^R, \mathbf{x}^S) \stackrel{\text{def}}{=} \int_{\mathbf{x}_T \in \mathbb{R}^2} \left[ \hat{v}_3^{(1)}(\mathbf{x}_T, x_3^{tl}; \mathbf{x}^R) \hat{p}^{(2)}(\mathbf{x}_T, x_3^{tl}; \mathbf{x}^S) - \hat{p}^{(1)}(\mathbf{x}_T, x_3^{tl}; \mathbf{x}^R) \hat{v}_3^{(2)}(\mathbf{x}_T, x_3^{tl}; \mathbf{x}^S) \right] d\mathbf{x}_T. \quad (3)$$

(Fokkema et al. (1999), Dillen et al. (2000a), Dillen (2000b)), in which the source positions of the respective wave fields are indicated. The integration is with respect to the transverse coordinate

$\mathbf{x}_T$ , at a depth  $x_3^{\text{tl}}$ . In Wapenaar (2000) applications of a similar boundary integral in terms of one-way wave fields are presented. In the following section the boundary integral of Eq. (3) is evaluated numerically.

### Numerical example

We consider the two-dimensional model shown in Fig. 2(a), with coordinate vector  $\mathbf{x} = (x_1, x_3)$ , in which  $x_1$  denotes the lateral position in terms of source-receiver offset, and  $x_3$  denotes depth (no  $x_2$  dependency). The wave fields are calculated and displayed in the time domain. The reference and monitor velocities and densities are given in Table 1. The reference and monitor sources are placed at the top of the model at 0 m depth, at 0 m offset. The receivers for both experiments are placed at 0 m depth, at offsets covering the entire model. Fig. 2(b) shows a difference gather obtained by subtracting a single reference shot-gather from a single monitor shot-gather. We proceed by computing the interaction integral of Eq. (3) at  $x_3^{\text{tl}} = 650$  m, i.e. between the diamond-shaped object and the lower layer, for  $(x_1^{\text{S}}, x_3^{\text{S}}) = (0, 0)$  m, and  $x_1^{\text{R}}$  ranging over the entire model and  $x_3^{\text{R}} = 0$  m. The result is shown in Fig. 2(c), for a selected range of  $x_1^{\text{R}}$  values. Next, the monitor model is changed such that it equals the reference model for  $x_3 < 650$  m, thereby eliminating the temporal contrast in the diamond-shaped object and retaining the temporal contrasts in the lower layer. The resulting difference gather, using the same source/receiver parameters with which Fig. 2(b) is obtained, is shown in Fig. 2(d). The difference reflections associated with the temporal contrast in the diamond-shaped object, visible in Fig. 2(b) have disappeared in Fig. 2(d). Note the similarity of Fig. 2(d) with Fig. 2(c), thereby indicating that the interaction integral is equivalent to a difference wave field which shows no temporal contrast above the interaction depth. In the remaining sections the boundary integral is investigated analytically.

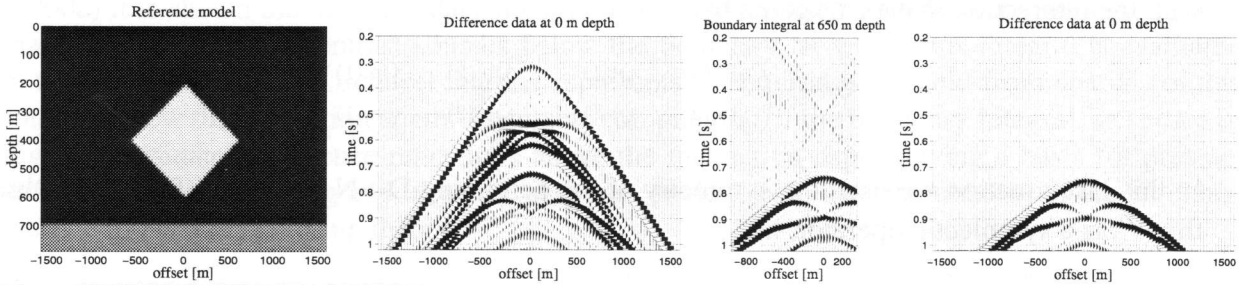


Figure 2: (a) Model containing a diamond-shaped object, embedded in a background medium, and a lower layer. Temporal contrast in diamond-shaped object and lower layer. (b) Difference wave field evaluated at  $x_3 = 0$  m depth for a range of offsets covering the model. (c) Interaction integral of Eq. (3) at  $x_3^{\text{tl}} = 650$  m. (d) Difference wave field at  $x_3 = 0$  m, no temporal contrasts for  $x_3 < 650$  m.

	$c^{(1)}$ [m/s]	$\rho^{(1)}$ [kg/m <sup>3</sup> ]	$c^{(2)}$ [m/s]	$\rho^{(2)}$ [kg/m <sup>3</sup> ]
background	1800	1500	1800	1500
diamond-shaped object	2500	2000	2700	2200
lower layer	2700	2300	2900	2400

Table 1: Reference and monitor velocities and densities,  $c^{(1)}, \rho^{(1)}, c^{(2)}$  and  $\rho^{(2)}$ .

### Wave field decomposition

In  $\mathbb{R}^3$  the *background* medium parameters,  $\{\rho^{\text{b}}, \kappa^{\text{b}}\}$ , are defined with respect to the actual medium parameters,  $\{\rho, \kappa\}$ , through the perturbation,  $\{\Delta\rho, \Delta\kappa\}$ , according to

$$\{\rho, \kappa\} = \{\rho^{\text{b}}, \kappa^{\text{b}}\}, \quad \text{in } \mathbb{D}^{\text{u}}, \quad \{\rho, \kappa\} = \{\rho^{\text{b}}, \kappa^{\text{b}}\} + \{\Delta\rho, \Delta\kappa\} \quad \text{in } \mathbb{D}^{\text{d}}, \quad (4)$$

(Fig. 1). Inside  $\mathbb{D} = \{(\mathbf{x}_T, x_3) | \mathbf{x}_T \in \mathbb{R}^2, \max(x_3^{\text{R}}, x_3^{\text{S}}) \leq x_3 \leq x_3^{\text{tl}}\}$  the actual wave field,  $\{\hat{p}, \hat{v}_k\}$  also denoted as the *total* wave field, is decomposed into a *down-going* wave field,  $\{\hat{p}^{\text{d}}, \hat{v}_k^{\text{d}}\}$ , and an *up-going* wave field,  $\{\hat{p}^{\text{u}}, \hat{v}_k^{\text{u}}\}$ , as

$$\hat{p} = \hat{p}^{\text{d}} + \hat{p}^{\text{u}} \quad \text{and} \quad \hat{v}_k = \hat{v}_k^{\text{d}} + \hat{v}_k^{\text{u}}, \quad \text{with} \quad \hat{v}_3^{\text{d}} = \hat{y}^{\text{b}} \hat{p}^{\text{d}} \quad \text{and} \quad \hat{v}_3^{\text{u}} = -\hat{y}^{\text{b}} \hat{p}^{\text{u}}. \quad (5)$$

The operators  $\pm\hat{\mathcal{Y}}^b$  are *Dirichlet-to-Neumann* operators which map a pressure function to the longitudinal component of a particle velocity function. The wave field decomposition of Eq. (5) follows from a particular normalisation of the incident and scattered wave fields associated with the perturbation of Eq. (4). One can show that (Dillen 2000b)

$$\hat{\mathcal{Y}}^b = \left(\hat{\mathcal{S}}^b\right)^{-1} \quad \text{and} \quad \hat{\mathcal{S}}^b = \left(\hat{\mathcal{S}}^b\right)^t, \quad (6)$$

in which  $^t$  signifies the transpose operation. The symmetric *single-layer potential* operator  $\hat{\mathcal{S}}^b$  is given by

$$\hat{\mathcal{S}}^b f(\mathbf{x}_T, x_3) = 2 \int_{\mathbf{x}'_T \in \mathbb{R}^2} \hat{G}^{q,b}(\mathbf{x}_T, x_3; \mathbf{x}'_T, x_3) f(\mathbf{x}'_T, x_3) d\mathbf{x}'_T, \quad (7)$$

with  $f \in L^2(\mathbb{R}^2)$ , and  $\hat{G}^{q,b}$  being the Green's functions with respect to the background medium. The integral symbol in this last definition signifies a Cauchy principal value integral.

### Interaction operator

Substituting Eq. (5) into the interaction quantity  $\hat{I}^{\text{conv}}$  of Eq. (3) yields

$$\hat{I}^{\text{conv}}(x_3^{\text{tl}}) = \int_{\mathbf{x}_T \in \mathbb{R}^2} \begin{pmatrix} \hat{p}^{\text{d},(1)} \\ \hat{p}^{\text{u},(1)} \end{pmatrix}^t(\mathbf{x}_T, x_3^{\text{tl}}) \hat{\mathcal{Y}}^b \begin{pmatrix} \hat{p}^{\text{d},(2)} \\ \hat{p}^{\text{u},(2)} \end{pmatrix}(\mathbf{x}_T, x_3^{\text{tl}}) d\mathbf{x}_T, \quad (8)$$

with the interaction matrix  $\hat{\mathcal{Y}}^b$  given by

$$\hat{\mathcal{Y}}^b = \begin{pmatrix} \hat{\mathcal{Y}}^{\text{b},(2)} - \hat{\mathcal{Y}}^{\text{b},(1)} & -\hat{\mathcal{Y}}^{\text{b},(2)} - \hat{\mathcal{Y}}^{\text{b},(1)} \\ \hat{\mathcal{Y}}^{\text{b},(2)} + \hat{\mathcal{Y}}^{\text{b},(1)} & -\hat{\mathcal{Y}}^{\text{b},(2)} + \hat{\mathcal{Y}}^{\text{b},(1)} \end{pmatrix}. \quad (9)$$

In this last equation we used the symmetry of the pertaining D-t-N operators (Eq. (6)). Observe that  $\hat{\mathcal{Y}}^b$  is a symplectic operator, i.e.

$$\left(\hat{\mathcal{Y}}^b\right)^t \mathbf{J} + \mathbf{J} \hat{\mathcal{Y}}^b = \mathbf{O} \quad \text{with} \quad \mathbf{J} = \begin{pmatrix} \mathcal{O} & \mathcal{I} \\ -\mathcal{I} & \mathcal{O} \end{pmatrix}, \quad (10)$$

in which  $\mathbf{J}$  is the *standard alternating* matrix,  $\mathbf{O}$  is the null matrix operator, and  $\mathcal{O}$  and  $\mathcal{I}$  are the scalar null and identity operators, respectively. Suppose that there are no temporal contrasts above the interaction depth  $x_3^{\text{tl}}$ , i.e. inside the upper half-space  $\mathbb{D}^u$  (Fig. 1). Then, the interaction matrix becomes skew-symmetric, according to

$$\hat{\mathcal{Y}}^b \Big|_{\{\rho^{\text{b},(1)}, \kappa^{\text{b},(1)}\} = \{\rho^{\text{b},(2)}, \kappa^{\text{b},(2)}\}} = \begin{pmatrix} \mathcal{O} & -2\hat{\mathcal{Y}}^b \\ 2\hat{\mathcal{Y}}^b & \mathcal{O} \end{pmatrix} \quad \text{with} \quad \hat{\mathcal{Y}}^b = \hat{\mathcal{Y}}^{\text{b},(1)} = \hat{\mathcal{Y}}^{\text{b},(2)}. \quad (11)$$

Also, one can show that for a  $\hat{q}$  source,

$$\hat{I}^{\text{conv}}(x_3^{\text{tl}}; \mathbf{x}^R, \mathbf{x}^S) \Big|_{\{\rho^{\text{b},(1)}, \kappa^{\text{b},(1)}\} = \{\rho^{\text{b},(2)}, \kappa^{\text{b},(2)}\}} = \hat{q}^{(1)} \hat{p}^{(2)}(\mathbf{x}^R; \mathbf{x}^S) - \hat{q}^{(2)} \hat{p}^{(1)}(\mathbf{x}^R; \mathbf{x}^S). \quad (12)$$

Hence, if there are no temporal contrasts in the density and the compressibility above the interaction depth  $x_3^{\text{tl}}$ ,  $\hat{\mathcal{Y}}^b$  becomes a skew-symmetric matrix, associated with a difference wave field evaluated at the recording depth. The appearance of  $\hat{I}^{\text{conv}}$  in Fig. 2(c), as compared to the difference wave field in Fig. 2(d), suggests that  $\hat{\mathcal{Y}}^b$  of Eq. (9), for nonvanishing temporal contrasts in the upper half-space  $\mathbb{D}^u$ , can be expressed in skew-symmetric form using a symplectic eigenvalue

decomposition. Exploiting the weak property of Eq. (11), that a sufficient condition for  $\hat{Y}^b$  to become skew-symmetric is the equality of the reference and monitor D-t-N operators, one obtains a symplectic eigenvalue decomposition of  $\hat{Y}^b$ . Implementing this decomposition one can show that (Dillen 2000b)

$$\hat{I}^{\text{conv}}(x_3^{\text{tl}}) = \int_{\mathbf{x}_T \in \mathbb{R}^2} \begin{pmatrix} \hat{p}^{\text{d},(1)'} \\ \hat{p}^{\text{u},(1)'} \end{pmatrix}^t(\mathbf{x}_T, x_3^{\text{tl}}) \hat{Y}^{\text{tl}} \begin{pmatrix} \hat{p}^{\text{d},(2)'} \\ \hat{p}^{\text{u},(2)'} \end{pmatrix}(\mathbf{x}_T, x_3^{\text{tl}}) d\mathbf{x}_T, \quad (13)$$

in which the primed wave constituents are given with respect to the symplectic basis, and in which the skew-symmetric matrix of symplectic eigenvalue operators is given by

$$\hat{Y}^{\text{tl}} = \begin{pmatrix} \mathcal{O} & -2\hat{Y}^{\text{tl}} \\ 2\hat{Y}^{\text{tl}} & \mathcal{O} \end{pmatrix} \quad \text{with} \quad \hat{Y}^{\text{tl}} = \left( \hat{Y}^{\text{b},(2)} \hat{Y}^{\text{b},(1)} \right)^{\frac{1}{2}}. \quad (14)$$

On this new basis we have the following wave field decomposition,

$$\hat{p} = \hat{p}^{\text{d}'} + \hat{p}^{\text{u}'} \quad \text{and} \quad \hat{v}_k = \hat{v}_k^{\text{d}'} + \hat{v}_k^{\text{u}'}, \quad \text{with} \quad \hat{v}_3^{\text{d}'} = \hat{Y}^{\text{tl}} \hat{p}^{\text{d}'} \quad \text{and} \quad \hat{v}_3^{\text{u}'} = -\hat{Y}^{\text{tl}} \hat{p}^{\text{u}'}, \quad (15)$$

## Discussion

The association of skew-symmetry of the interaction matrix (see Eq. (11)) with a difference wave field (see Eq. (12)), is extended to the case where temporal contrasts are present above the interaction depth  $x_3^{\text{tl}}$ , using a symplectic eigenvalue decomposition of the interaction matrix of Eq. (9). On the new basis the reference and monitor D-t-N operators, and consequently the wave field decomposition operations, are equal, and given by Eqs. (14) and (15), although the background reference and monitor densities and compressibilities, and velocities, may be unequal. In Dillen (2000a) it is shown that the boundary integral of Eq. (3) represents a difference wave field, originating from temporal contrast sources below the boundary, at which this integral is evaluated, in the same way as the Kirchhoff integral represents a scattered wave field from spatial contrast sources below the evaluation depth. Recursive computation of the boundary integral, as shown by Fig. 3, eliminates difference reflections above the interaction depth, giving a basis for prestack temporal contrast imaging and inversion schemes, analogous to implementations of the Kirchhoff integral in inverse scattering theory.

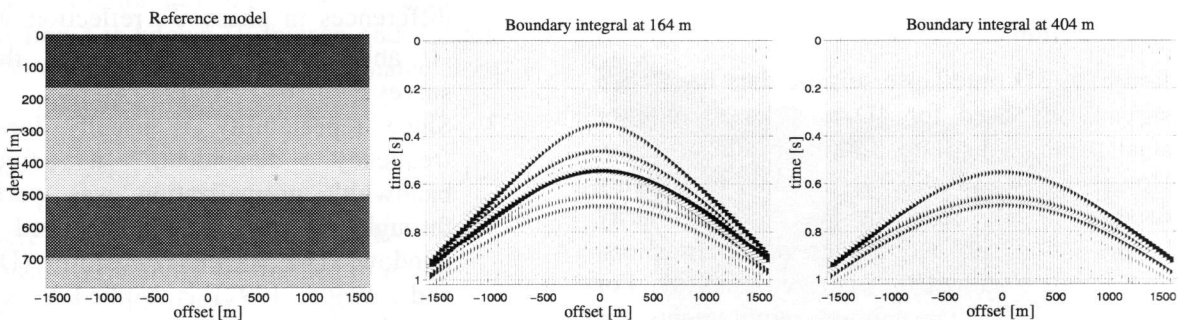


Figure 3: (a) Layered model with time-lapse differences in first, third and fifth layer, (b) interaction integral of Eq. (3) at  $x_3^{\text{tl}} = 164$  m, and at (c)  $x_3^{\text{tl}} = 404$  m.

## References

- J.T. Fokkema, C.P.A. Wapenaar, and M.W.P. Dillen, *Reciprocity theorems for time-lapse seismics*, 6th SBGF meeting, Rio de Janeiro, 1999, Abstract 325.
- C.P.A. Wapenaar, J.T. Fokkema, M.W.P. Dillen, and P. Scherpenhuijsen, *One-way acoustic reciprocity and its applications in multiple elimination and time-lapse seismics*, SEG 70th Ann. Int. Mtg., Calgary, 2000, Expanded Abstracts, pp 2377-2380.
- M.W.P. Dillen, J.T. Fokkema, and C.P.A. Wapenaar, *Convolution type interaction of time-lapse acoustic wave fields*, SEG 70th Ann. Int. Mtg., Calgary, 2000a, Expanded Abstracts, pp 2381-2384.
- M.W.P. Dillen, *Time-lapse seismic monitoring of subsurface stress dynamics*, Ph.D. thesis Delft University of technology, 2000b.